Plasma Pharmacokinetics, Whole-Body Distribution, Metabolism, and Radiation Dosimetry of ^{68}Ga Bombesin Antagonist BAY 86-7548 in Healthy Men

Anne Roivainen[1], Esa Kähkönen[2], Pauliina Luoto[1], Sandra Borkowski[3], Birte Hofmann[3], Ivan Jambor[1], Kaisa Lehtiö[1,4], Tuija Rantala[1], Antje Rottmann[3], Henri Sipilä[1], Rick Sparks[5], Sami Suilamo[1,4], Tuula Tolvanen[1], Ray Valencia[3], and Heikki Minn[1,4]

[1]Turku PET Centre, University of Turku and Turku University Hospital, Turku, Finland; [2]Department of Urology, Turku University Hospital, Turku, Finland; [3]Bayer HealthCare Pharmaceuticals, Bayer Pharma AG, Berlin, Germany; [4]Department of Oncology and Radiotherapy, Turku University Hospital, Turku, Finland; and [5]CDE Dosimetry Services, Inc., Knoxville, Tennessee

This first-in-human study investigated the safety, tolerability, metabolism, pharmacokinetics, biodistribution, and radiation dosimetry of ^{68}Ga-bombesin antagonist ^{68}Ga-DOTA-4-amino-1-carboxymethylpiperidine-D-Phe-Gln-Trp-Ala-Val-Gly-His-Sta-Leu-NH_2 (BAY 86-7548). **Methods:** Five healthy men underwent dynamic whole-body PET/CT after an intravenous injection of BAY 86-7548 (138 ± 5 MBq). Besides total radioactivity, plasma samples were analyzed by radio–high-performance liquid chromatography for metabolism of the tracer. Dosimetry was calculated using the OLINDA/EXM software. **Results:** Three radioactive plasma metabolites were detected. The proportion of unchanged BAY 86-7548 decreased from 92% ± 9% at 1 min after injection to 19% ± 2% at 65 min. The organs with the highest absorbed doses were the urinary bladder wall (0.62 mSv/MBq) and the pancreas (0.51 mSv/MBq). The mean effective dose was 0.051 mSv/MBq. BAY 86-7548 was well tolerated by all subjects. **Conclusion:** Intravenously injected BAY 86-7548 is safe, and rapid metabolism is demonstrated. A 150-MBq injection of BAY 86-7548 results in an effective dose of 7.7 mSv, which could be reduced to 5.7 mSv with frequent bladder voids.

Key Words: dosimetry; ^{68}Ga; PET; pharmacokinetics; radiometabolism; whole-body distribution

J Nucl Med 2013; 54:867–872
DOI: 10.2967/jnumed.112.114082

Prostate cancer (PCa) is the second most common cancer in men globally (*1*) and the most common cancer in developed countries (*2*). However, conventional imaging techniques such as ultrasound, contrast-enhanced CT, or MR imaging have limited sensitivity and specificity for detecting primary, metastatic, and recurrent PCa (*3*). PET/CT plays an important role in the attempt to improve and individualize therapeutic approaches in oncology. The most widely used tracer, ^{18}F-FDG, shows a high excretion in the urinary bladder and demonstrates generally an unsatisfactory uptake in PCa, especially in the early phase (*4,5*). Tracers that depict lipid metabolism such as ^{11}C-choline and ^{11}C-acetate have already been applied for imaging PCa, but they accumulate also in prostatic hyperplasia, with overlapping uptake in benign and malignant intraprostatic lesions (*6–8*). Consequently, there is an urgent need for more PCa-specific tracers.

Gastrin-releasing peptide receptors (GRPr) are highly overexpressed in a variety of human tumors including PCa (*9*). Preclinical data suggest the possibility of a high PCa-specific signal with radiolabeled bombesin analogs targeting GRPr (*10*). These analogs could potentially provide better and more specific diagnosis than ^{18}F-FDG or tracers such as ^{11}C-choline or ^{11}C-acetate.

^{68}Ga-DOTA-4-amino-1-carboxymethylpiperidine-D-Phe-Gln-Trp-Ala-Val-Gly-His-Sta-Leu-NH_2 (BAY 86-7548; also known as RM2) is a bombesin antagonist with high GRPr affinity. The purpose of this first-in-human study was to investigate the safety, tolerability, metabolism, pharmacokinetics, biodistribution, and radiation dosimetry of BAY 86-7548 in healthy volunteers receiving an intravenous injection of this antagonist.

MATERIALS AND METHODS

Further method details are presented in the supplemental data (available online only at http://jnm.snmjournals.org).

Radiochemistry

The radiosynthesis of BAY 86-7548 was performed under good manufacturing practices with an automated synthesis module (Modular Lab IGG-100; Eckert & Ziegler).

Subjects

Five healthy men (mean age ± SD, 52 ± 2 y; mean weight ± SD, 77 ± 10 kg; mean height ± SD, 172 ± 5 cm) were enrolled in the study, which was approved by the Ethics Committee and by the Finnish Medicines Agency. None of these 5 subjects had significant findings on routine blood tests, electrocardiography, and

Received Sep. 28, 2012; revision accepted Dec. 28, 2012.
For correspondence or reprints contact: Anne Roivainen, Turku PET Centre, Kiinamyllynkatu 4-8, FI-20521 Turku, Finland.
E-mail: anne.roivainen@utu.fi
Published online Apr. 5, 2013.
COPYRIGHT © 2013 by the Society of Nuclear Medicine and Molecular Imaging, Inc.

physical examination or had a history of alcohol or drug abuse. Each subject signed a written informed consent before entering the study. After consent, they underwent a digital rectal examination with transrectal ultrasound, and no suggestive findings were revealed. The mean prostate volume was 17.2 ± 7.8 mL. During the imaging, the vital signs of the subjects were monitored, including a 12-lead electrocardiography. Blood and urine were analyzed before and after PET/CT scanning.

PET/CT

Imaging was performed on a Discovery VCT PET/CT device (GE Healthcare). BAY 86-7548 (138 ± 5 MBq, 7 ± 1 mL, 20 ± 4 μg) was intravenously injected as a bolus, and PET scanning started at 1, 10, 20, 40, 100, and 200 min after injection. The acquisition times per bed position were 30, 60, 120, 180, 300, and 360 s. The first scan for each subject included 14 bed positions (head to toes), and other scans had 8 bed positions (head to mid thighs). PET images were reconstructed using a 3-dimensional VUE Point algorithm (GE Healthcare) with 2 iterations, 28 subsets, and a postprocessing filter of 3 mm in full width at half maximum. The final in-plane resolution was 5 mm (*11*).

Dosimetry

Regions of interest were constructed on coronal slices to create volumes of interest representing radioactivity-containing organs or tissues. Where reasonable, some coronal slices were combined before region-drawing to reduce the number of regions of interest required to complete this process. Radioactivities in the member voxels were determined using the direct concentration results from the images, along with the volumes of the voxels. The total radioactivity in each radioactivity-containing organ or tissue was calculated by a simple summation of the radioactivities in the member voxels. This process was repeated at all imaging times to create time–activity data. Urinary excretion time–activity data were estimated using both image-based estimation and urinary void measurement.

The fraction of total injected radioactivity form of time–activity data were modeled using sums of exponentials, with between 1 and 4 exponentials, as required. The resultant models were integrated to produce a normalized number of disintegrations in units of hours.

Data modeling, estimation of normalized number of disintegrations, and production of dosimetry estimates were performed using the RADAR (RAdiation Dose Assessment Resource) method for internal dosimetry as implemented in the OLINDA/EXM (version 1.1) software (*12*). All of these methods, including the image quantification, were also in general concordance with the methodology and principles as presented in the MIRD 16 document (*13*). The adult male phantom (~70 kg) reference model was used. A urinary bladder–voiding interval of 3.5 h was used. For salivary glands, a conservative dose factor for a single sphere (based on the combined mass of the salivary glands) was used to determine the self-dose component of the salivary gland–absorbed doses. On the basis of the photon component of brain dose (self- and cross-photon irradiation), cross-irradiation would likely contribute significantly less than 10% of the total salivary gland–absorbed dose. The salivary dose reported here is self-dose only.

Metabolism and Pharmacokinetics

Venous blood samples were drawn during a period of 1–150 min after injection of BAY 86-7548. The radioactivity of blood and plasma were measured with a γ-counter. The plasma samples were also analyzed by radio–high-performance liquid chromatography (radio-HPLC) for intact BAY 86-7548 and radioactive metabolites, and metabolite-corrected plasma time–activity curves were used for the calculation of pharmacokinetic parameters.

The structure of the metabolites was elucidated by the incubation of the test compound BAY 86-7549 containing stable $^{69/71}$Ga with human hepatocytes, and then by comparison of the resulting liquid chromatography–mass spectrometry data with human plasma radiochromatograms.

Statistical Analyses

The arithmetic mean values were calculated from the individual measurements and expressed at a precision of 1 SD (mean ± SD).

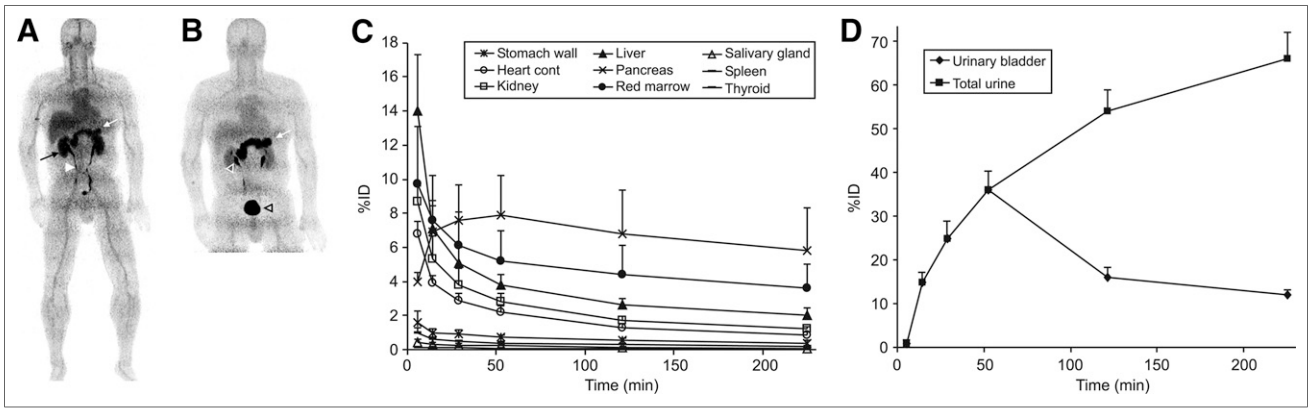

FIGURE 1. Coronal PET images of a healthy volunteer (man; age, 53 y; weight, 76 kg; height, 176 cm) after intravenous injection of 140 MBq of BAY 86-7548. (A) Distribution of ^{68}Ga radioactivity at 1–7 min after injection, as imaged for 30 s/bed position, shows high uptake predominantly in pancreas (white arrow), kidneys (black arrow), and ureter (white arrowhead). (B) At 10–18 min after injection, as imaged for 60 s/bed position, uptake is mainly in pancreas (white arrow), renal pelvis (white transparent arrowhead), and urinary bladder (black transparent arrowhead). Mean percentage injected dose as function of time of main organs (C) and urinary bladder and total urine (D) of all subjects. Error bars denote SD values. %ID = percentage injected dose.

TABLE 1
Normalized Number of Disintegrations (Hours) of Source Organs After Injection of BAY 86-7548

Organ	Mean	SD	Minimum	Maximum
Heart contents	0.038	0.0052	0.029	0.043
Kidneys	0.050	0.0071	0.041	0.060
Liver	0.074	0.014	0.055	0.093
Pancreas	0.11	0.035	0.067	0.15
Red marrow	0.087	0.030	0.066	0.11
Salivary	0.0033	0.0013	0.0011	0.0044
Spleen	0.0065	0.0014	0.0040	0.0073
Stomach wall	0.012	0.0030	0.0079	0.014
Thyroid	0.0012	0.00054	0.0057	0.0018
Urinary bladder	0.53	0.050	0.47	0.59
Remainder of body	0.67	0.071	0.59	0.75

RESULTS

Radiochemistry

The BAY 86-7548 was obtained with moderate yield (452 ± 85 MBq, $n = 5$). Radioactivity concentration, specific radioactivity, and radiochemical purity were 43 ± 9 MBq/mL, 26 ± 5 GBq/μmol, and greater than 98%, respectively.

Biodistribution and Dosimetry

The ^{68}Ga radioactivity was rapidly excreted through the kidneys to the urinary bladder and accumulated predominantly in the pancreas and liver (Fig. 1). Maximum peak uptake of the total injected radioactivity was seen in the urinary bladder contents and the liver, with approximately 36% and 14%, respectively.

The mean normalized number of disintegrations in units of hours of the source organs and remainder of the body are listed in Table 1. The largest mean normalized number of disintegrations for the subjects was found in the remainder tissues (0.67 h), urinary bladder contents (0.53 h), and pancreas (0.11 h).

The estimations of the absorbed doses are reported in Table 2. The organ with the highest absorbed dose was the urinary bladder wall at 0.61 mSv/MBq, followed by the pancreas at 0.51 mSv/MBq. The mean effective dose (*14*) was 0.051 mSv/MBq. Thus, the effective dose from

TABLE 2
Dose Equivalent Estimates (mSv/MBq) After Injection of BAY 86-7548

Organ	Mean	SD	Minimum	Maximum
Adrenals	0.011	0.00080	0.010	0.012
Brain	0.0056	0.00051	0.0049	0.0061
Breasts	0.0060	0.00048	0.0053	0.0064
Gallbladder wall	0.011	0.00054	0.0099	0.011
Lower large intestine wall	0.014	0.00036	0.013	0.014
Small intestine	0.010	0.00032	0.0096	0.010
Stomach wall	0.038	0.0090	0.027	0.045
Upper large intestine wall	0.0094	0.00037	0.0089	0.0098
Heart wall	0.028	0.0030	0.023	0.031
Kidneys	0.081	0.011	0.067	0.096
Liver	0.023	0.0035	0.019	0.028
Lungs	0.0071	0.00048	0.0064	0.0076
Muscle	0.0082	0.00038	0.0077	0.0086
Pancreas	0.51	0.16	0.32	0.73
Red marrow	0.013	0.0087	0.0068	0.026
Osteogenic cells	0.013	0.0051	0.0092	0.021
Salivary glands	0.022	0.0022	0.020	0.026
Skin	0.0060	0.00044	0.0055	0.0065
Spleen	0.023	0.0036	0.017	0.026
Testes	0.010	0.00045	0.0097	0.011
Thymus	0.0070	0.00055	0.0064	0.0076
Thyroid	0.027	0.011	0.014	0.039
Urinary bladder wall	0.61	0.057	0.54	0.68
Total body	0.010	0.00031	0.0098	0.011
Effective dose	0.051	0.0072	0.044	0.063

a 150-MBq injected radioactivity is 7.7 mSv, which could be reduced to roughly 5.7 mSv with frequent bladder voiding (1-h voids).

BAY 86-7548 was well tolerated by all subjects.

Metabolism and Pharmacokinetics

The proportion of intact BAY 86-7548 on total radioactivity in venous plasma declined rapidly, and 3 metabolites were detected by radio-HPLC. Typical radio-HPLC chromatograms are shown in Figure 2. The proportions of unchanged BAY 86-7548 were 92% ± 9%, 68% ± 9%, 47% ± 6%, 29% ± 6%, 19% ± 2%, 16% ± 4%, and 15% ± 2% at 1, 10, 20, 40, 65, 100, and 150 min after injection, respectively.

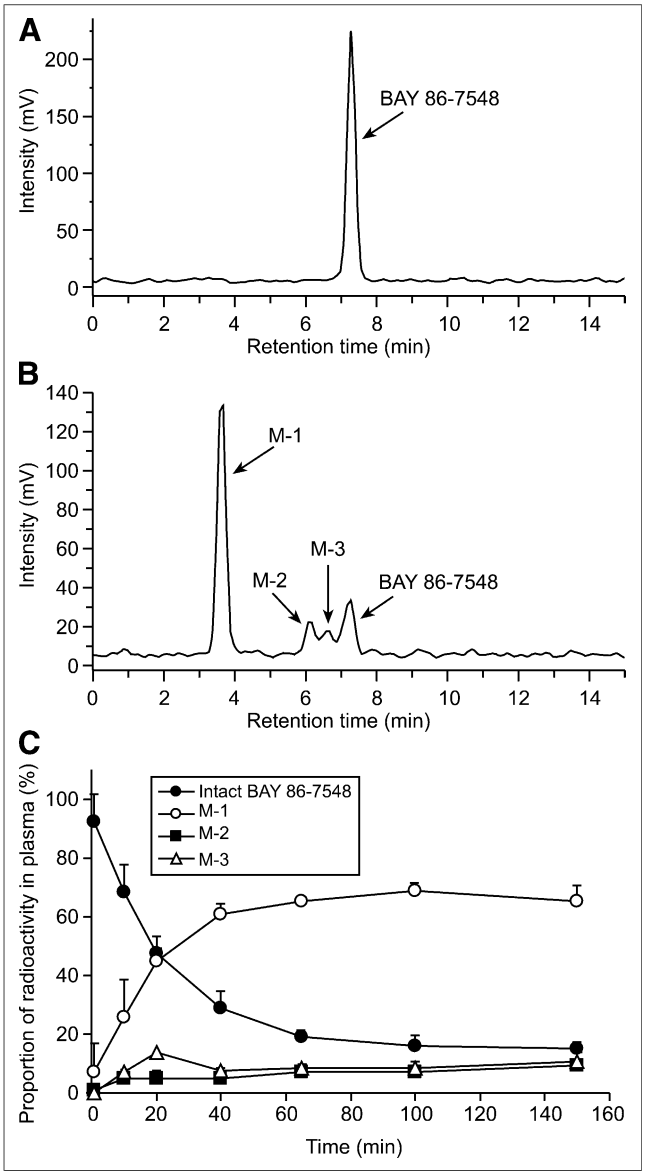

FIGURE 2. Representative radio-HPLC chromatograms of intact BAY 86-7548 (A) and human plasma (B) at 65 min after injection. After intravenous injection of BAY 86-7548 to healthy volunteers, 3 radiometabolites were detected in human plasma by radio-HPLC. (C) Proportion of parent tracer decreased rapidly in blood circulation.

The in vitro investigations applying human hepatocytes revealed the metabolic pathways, which are presented in Figure 3. Metabolite M-1 (^{68}Ga-DOTA chelate) appeared to be major, and M-2 (cleavage of amide bond at alanine–valine) and M-3 (hydrolysis of glutamine residue) were minor constituents of total radioactivity.

The plasma pharmacokinetic parameters are summarized in Table 3. The unchanged tracer reached maximum plasma concentration after about 10 min and was eliminated from the circulation, with a terminal half-life of about 80 min. The total clearance was estimated to be about 55 L/h.

Further results details are presented in the supplemental data.

DISCUSSION

BAY 86-7548 is a promising novel PET tracer for the imaging of GRPr, which is overexpressed in several tumors, such as PCa. This study describes the whole-body distribution and radiation dosimetry of BAY 86-7548. Its metabolic fate and pharmacokinetics in healthy humans were also evaluated.

Intravenously administered BAY 86-7548 demonstrated fast renal clearance, which is connected to the hydrophilic properties and the small size of the peptide. The highest radioactivity uptake was detected in the pancreas, which is in the line with the expression GRPr (*15*) and previous preclinical studies with RM2 peptide (*10*). The radioactive metabolites of BAY 86-7548 may contribute to the liver and bone marrow uptake, although the extent of this contribution is not known.

The image quantification and dosimetry results were consistent across the subject population. Although ^{68}Ga has been used extensively for the labeling of synthetic peptides, human dosimetry data are available only from peptide analogs that bind to somatostatin receptors or $\alpha_v\beta_3$ integrin. The effective dose of BAY 86-7548 reported here (0.051 mSv/MBq) is comparable but slightly higher than those of ^{68}Ga-DOTATOC (0.023 mSv/MBq), ^{68}Ga-DOTANOC (0.025 mSv/MBq), and ^{68}Ga-NOTA-RGD (0.022 mSv/MBq) (*16–18*). The effective dose of ^{18}F-FDG is 0.019 mSv/MBq according to the International Commission on Radiological Protection, publication 106 (*19*). Thus, the effective dose ratio of BAY 86-7548 to ^{18}F-FDG was 2.7.

BAY 86-7548 showed rapid blood clearance, which is commonly due to fast renal excretion. Unchanged BAY 86-7548 and 3 metabolites (M-1, M-2, and M-3) were detected in the radiochromatograms of human plasma. Additional metabolites, which might be considered as major, were not identified in the course of the investigations. According to the guidelines of the International Conference on Harmonisation of Technical Requirements for Registration of Pharmaceuticals for Human Use (ICH Topic M 3 (R2)), the exposure cutoff for major metabolites of interest is defined as 10% of total drug-related exposure (*20*). In line with this definition, metabolite M-1 has to be considered as a major metabolite, whereas metabolites M-2 and M-3 are regarded as minor metabolites.

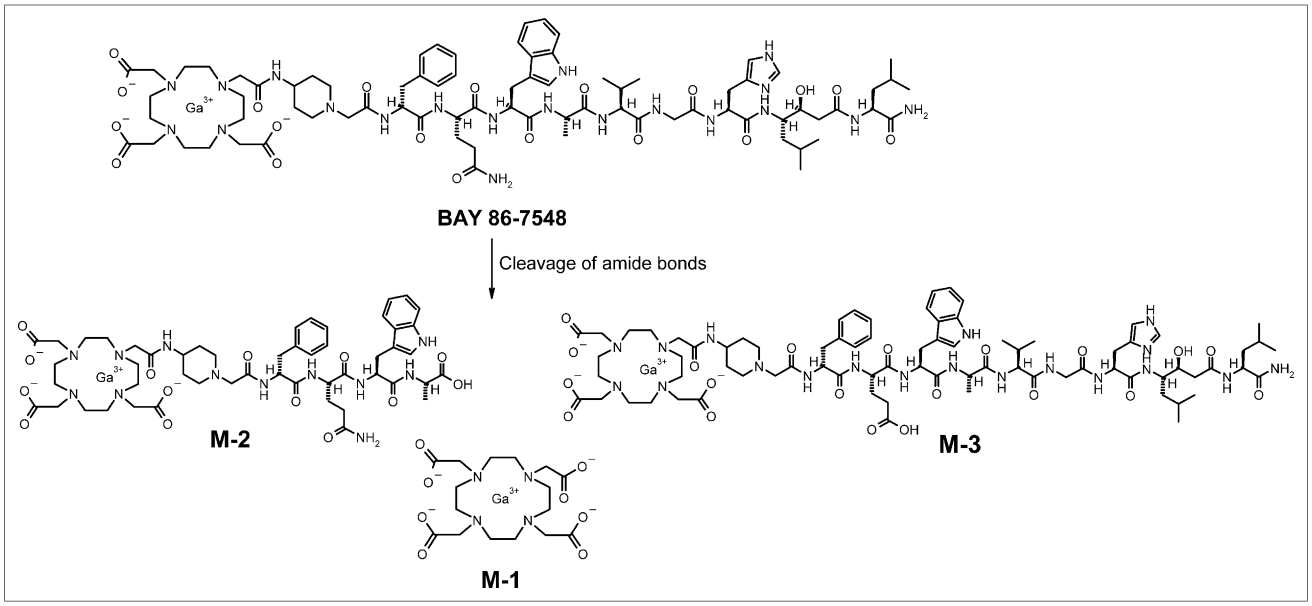

FIGURE 3. Major metabolic pathways of BAY 86-7548. Cleavage of amide bond at alanine–valine and at glutamine residue was confirmed by liquid chromatography–mass spectrometry of metabolites present in human hepatocytes. However, polar metabolite M-1 in human plasma was not found in liver microsomes or hepatocytes. Analyses with DOTA chelate, as reference, revealed M-1 as ^{68}Ga-DOTA chelate.

CONCLUSION

Intravenously injected BAY 86-7548 was safe, and rapid metabolism was demonstrated in human blood circulation. The radiation burden due to BAY 86-7548 was comparable but slightly higher than that of the other ^{68}Ga peptides. From a radiation safety perspective, BAY 86-7548 imaging is feasible in applied clinical studies and can be performed in the same subjects multiple times per year. This repeatability is useful, for example, in trials aiming to clarify the treatment efficacy of novel drug candidates.

DISCLOSURE

The costs of publication of this article were defrayed in part by the payment of page charges. Therefore, and solely to indicate this fact, this article is hereby marked "advertisement" in accordance with 18 USC section 1734. This study was sponsored by Bayer Pharma AG, Berlin, Germany. Sandra Borkowski, Birte Hofmann, Anne Roivainen, and Ray Valencia are employees of Bayer HealthCare Pharmaceuticals, Bayer Pharma AG, Berlin, Germany. Rick Sparks is an employee of CDE Dosimetry Services, Inc., Knoxville, Tennessee. No other potential conflict of interest relevant to this article was reported.

ACKNOWLEDGMENTS

The professional assistance of the staff at Turku PET Centre is greatly appreciated. Robert M. Badeau is acknowledged for careful proofreading of this scientific manuscript.

TABLE 3
Plasma Pharmacokinetic Parameters After Intravenous Administration of BAY 86-7548

	Total radioactivity			Unchanged tracer				
Parameter	C_{max} (%ID/mL)	t_{max}* (min)	AUC(0-t_{last}) (%ID*min/mL)	C_{max} (pmol/L)	t_{max}* (min)	AUC(0-t_{last}) (pmol*h/L)	CL† (L/h)	$t_{1/2}$† (min)
Arithmetic mean	0.0106	10.6	0.0116	438	10.6	157	55.5	81.0
Arithmetic SD	0.00766	1.88	0.00174	380	1.88	46.6	12.8	21.5
Coefficient of variation (%)	72.6	11.0	15.0	86.8	11.0	29.7	23.1	26.5

*Median, minimum, and maximum are listed instead of arithmetic mean, SD, and coefficient of variation.
†Values have to be regarded as estimates, because sampling time was not sufficient to describe terminal elimination phase adequately.
Injected dose of BAY 86-7548 was 140 MBq (total mass ≤ 28 μg) and number of experiments 5.
C_{max} = maximum concentration; %ID = percentage injected dose; t_{max} = time of maximum; AUC = area under curve; CL = total clearance; $t_{1/2}$ = plasma half-life

REFERENCES

1. Ferlay J, Shin HR, Bray F, Forman D, Mathers C, Parkin DM. Estimates of worldwide burden of cancer in 2008: GLOBOCAN 2008. *Int J Cancer.* 2010; 127:2893–2917.
2. Siegel R, Naishadham D, Jemal A. Cancer statistics, 2012. *CA Cancer J Clin.* 2012;62:10–29.
3. Krause BJ, Souvatzoglou M, Tuncel M, et al. The detection rate of [^{11}C]Choline-PET/CT depends on the serum PSA-value in patients with biochemical recurrence of prostate cancer. *Eur J Nucl Med Mol Imaging.* 2008;35:18–23.
4. Liu IJ, Zafar MB, Lai YH, Segall GM, Terris MK. Fluorodeoxyglucose positron emission tomography studies in diagnosis and staging of clinically organ-confined prostate cancer. *Urology.* 2001;57:108–111.
5. Effert PJ, Bares R, Handt S, Wolff JM, Bull U, Jakse G. Metabolic imaging of untreated prostate cancer by positron emission tomography with ^{18}fluorine-labeled deoxyglucose. *J Urol.* 1996;155:994–998.
6. Jambor I, Borra R, Kemppainen J, et al. Functional imaging of localized prostate cancer aggressiveness using ^{11}C-acetate PET/CT and ^{1}H-MR spectroscopy. *J Nucl Med.* 2010;51:1676–1683.
7. Mena E, Turkbey B, Mani H, et al. ^{11}C-Acetate PET/CT in localized prostate cancer: a study with MR imaging and histopathologic correlation. *J Nucl Med.* 2012;53:538–545.
8. Souvatzoglou M, Weirich G, Schwarzenboeck S, et al. The sensitivity of [^{11}C] choline PET/CT to localize prostate cancer depends on the tumor configuration. *Clin Cancer Res.* 2011;17:3751–3759.
9. Reubi JC, Wenger S, Schmuckli-Maurer J, et al. Bombesin receptor subtypes in human cancers: detection with the universal radioligand ^{125}I-[D-TYR6, β-ALA11, PHE13, NLE14]Bombesin(6-14). *Clin Cancer Res.* 2002;8:1139–1146.
10. Mansi R, Wang X, Forrer F, et al. Development of a potent DOTA-conjugated bombesin antagonist for targeting GRPr-positive tumours. *Eur J Nucl Med Mol Imaging.* 2011;38:97–107.
11. Teräs M, Tolvanen T, Johansson JJ, Williams JJ, Knuuti J. Performance of the new generation of whole-body PET/CT scanners: Discovery STE and Discovery VCT. *Eur J Nucl Med Mol Imaging.* 2007;34:1683–1692.
12. Stabin MG, Sparks RB, Crowe EB. OLINDA/EXM: the second generation personal computer software for internal dose assessment in nuclear medicine. *J Nucl Med.* 2005;46:1023–1027.
13. Siegel JA, Thomas SR, Stubbs JB, et al. MIRD pamphlet no. 16: techniques for quantitative radiopharmaceutical biodistribution data acquisition and analysis for use in human radiation dose estimates. *J Nucl Med.* 1999;40(suppl):37S–61S.
14. International Commission on Radiological Protection (ICRP). *1990 Recommendations of the International Commission on Radiological Protection.* ICRP Publication 60. New York, NY: Pergamon Press; 1991.
15. Jensen RT, Battey JF, Spindel ER, et al. International union of pharmacology. LXVIII. Mammalian bombesin receptors: nomenclature, distribution, pharmacology, signaling, and functions in normal and disease states. *Pharmacol Rev.* 2008;60:1–42.
16. Hartmann H, Zöphel K, Freudenberg R, et al. Radiation exposure of patients during ^{68}Ga-DOTATOC PET/CT examinations. *Nuklearmedizin.* 2009;48:201–207.
17. Pettinato C, Sarnelli A, Di Donna M, et al. ^{68}Ga-DOTANOC: biodistribution and dosimetry in patients affected by neuroendocrine tumors. *Eur J Nucl Med Mol Imaging.* 2008;35:72–79.
18. Kim JH, Lee JS, Kang KW, et al. Whole-body distribution and radiation dosimetry of ^{68}Ga-NOTA-RGD, a positron emission tomography agent for angiogenesis imaging. *Cancer Biother Radiopharm.* 2012;27:65–71.
19. International Commission on Radiological Protection (ICRP). Radiation doses to patients from radiopharmaceuticals: a third amendment to ICRP publication 53. ICRP publication 106. *Ann ICRP.* 2008;38:1–198.
20. International Conference on Harmonisation; Guidance on M3(R2) nonclinical safety studies for the conduct of human clinical trials and marketing authorization for pharmaceuticals; availability. Notice. *Fed Regist.* 2010;75: 3471–3472.